RSC Advances

REVIEW

View Article Online
View Journal | View Issue

Cite this: *RSC Adv.*, 2025, **15**, 26184

Recent trends on MIL-88(Fe) metal–organic frameworks: synthesis and applications in pollutant removal and detection

Qinqin Gao, [a] Qinglin Sheng, [b] Sai Zhang *[a] and Yuping Tang*[a]

Plastic, pharmaceutical, and heavy metal pollution continues to escalate, creating an urgent need for efficient detection and removal of hazardous pollutants. Consequently, emerging technologies are critically required to advance environmental monitoring and remediation. Metal–organic frameworks (MOFs), as porous, flexible, and multifunctional materials with unique structural characteristics, offer viable solutions to these challenges, with MIL-88(Fe) serving as the central focus of this study. In this paper, we review the synthesis and applications of MIL-88(Fe): we summarize and compare its solvothermal, microwave-assisted, electrochemical, ultrasonic, and mechanochemical synthesis methods, and systematically review the removal and detection of organic pollutants, pharmaceuticals, and heavy metals by MIL-88(Fe) and its composites under varying conditions. MIL-88(Fe) exhibits notable advantages: it possesses a stable and tunable structure, enabling adaptation to complex environments; it demonstrates high adsorption capacity and detection sensitivity; it achieves high efficiency through mechanisms including coordination, electrostatic adsorption, and π–π stacking; and it is reusable, thereby reducing application costs. In conclusion, MIL-88(Fe) is a multifunctional material for environmental remediation, and its potential has been validated. Future research should focus on optimizing its performance, scaling up synthesis, integrating it with other materials and technologies, and enhancing environmental protection and pollution control.

Received 30th April 2025
Accepted 14th July 2025

DOI: 10.1039/d5ra03049h

rsc.li/rsc-advances

1 Introduction

The rapid pace of industrialization and urbanization has triggered severe environmental pollution, particularly in water resources.[1–3] However, the escalating contamination of water

[a]Key Laboratory of Shaanxi Administration of Traditional Chinese Medicine for TCM Compatibility, Shaanxi University of Chinese Medicine, Xi'an 712046, China. E-mail: zhangsai@sntcm.edu.cn; yupingtang@sntcm.edu.cn
[b]College of Food Science and Technology, Northwest University, Xi'an 710069, China

Qinqin Gao

Qinqin Gao is a graduate student at Shaanxi University of Chinese Medicine. Her primary research interests include electrochemical sensing, pharmaceutical analysis, and analytical chemistry. Under the supervision of her advisor, she focuses on developing greener synthetic routes for stable and highly porous metal–organic frameworks (MOFs), as well as their chemical modification, for applications in the electrochemical detection of pesticide residues in traditional Chinese medicines (TCMs).

Qinglin Sheng

Qinglin Sheng, PhD, holds positions including Deputy Secretary General of Shaanxi Agricultural Engineering Society and Director of Shaanxi Society of Food Science and Technology. He is a young editorial board member of several journals. He has received honors like "Shaanxi Young Rising Star of Science and Technology" and "Shaanxi Youth Science and Technology Award". His research focuses on food safety detection, electrochemical sensing, etc. He has led multiple research projects and published over 100 papers in journals like Analytical Chemistry, with 1 book and 7 authorized invention patents.

bodies by toxic chemicals, resulting from the continuous discharge of untreated industrial and domestic effluents, has become a pressing environmental concern.[4] As untreated, they pose serious threats to aquatic ecosystems and human health.[4] Several studies have reported that common pollutants—including heavy metals,[5] organic dyes, and pharmaceutical residues[6]—are becoming increasingly prevalent, along with their associated toxicities. Recent studies have highlighted several prevalent waterborne pollutants, including microcystins (MCs), disinfection by-products (DBPs), heavy metals (HMs), dioxins, and polychlorinated biphenyls (PCBs).[7] These contaminants pose significant threats to human health and ecosystems due to their toxicity, persistence, and potential for bioaccumulation.[8,9] For instance, CIT, a nephrotoxic and genotoxic compound, raises significant concerns regarding the safety of consuming CIT-contaminated food and feed.[10] Similarly, heavy metals like chromium, cadmium, copper, lead, and mercury have been widely reported for their toxic effects.[8]

If not properly treated, these pollutants can lead to severe health consequences, including the development of antibiotic-resistant genes in bacteria due to antibiotic contamination in water, which reduces the effectiveness of current antibiotic treatments.[11] Moreover, the presence of organic dyes in water reduces sunlight penetration, impairing photosynthesis in aquatic plants and microorganisms, and depleting the biochemical oxygen demand of water bodies, hindering the decomposition of organic compounds.[12] Emerging contaminants, such as microplastics, nanoplastics, and pharmaceutical and personal care products (PPCPs), further exacerbate the complexity of the pollution landscape.[13] Consequently, it is necessary to monitor and purify water sources before their safe utilization.

Current technologies for pollutant detection and removal present both advantages and inherent limitations. Conventional physical methods (*e.g.*, filtration, sedimentation) offer simplicity in operation but often lack selectivity for specific contaminants.[14] Chemical treatments, while effective for certain pollutants, may generate harmful byproducts and require significant energy input. Biological approaches utilizing microorganisms or enzymes demonstrate environmental friendliness; however, their application is limited by slow processing times and sensitivity to environmental conditions.[15] Advanced materials like graphite oxides and carbon nanotubes exhibit exceptional adsorption capacities, but their high production costs and potential secondary pollution limit large-scale implementation.[16,17] Similarly, while cyclodextrin-based systems show remarkable molecular recognition capabilities, their practical application is hindered by stability issues and the need for crosslinking agents.[18] These limitations highlight the critical need for innovative materials that combine high efficiency, selectivity, and sustainability.

Metal–Organic Frameworks (MOFs) or Porous Coordination Polymers (PCPs) are hybrid porous materials formed by the self-assembly of metal ions or clusters with multidentate organic linkers *via* coordination bonds.[19–21] They exhibit high specific surface areas, structural tunability, thermal/chemical stability, and versatile optical/electronic properties, showing promise in gas adsorption, catalysis (photocatalysis, electrocatalysis), chemical sensing, and gas separation.[22,23] Their unique host–guest interactions and multifunctionality make them ideal for designing high-performance materials.[24] However, common limitations exist: HKUST-1 and MOF-5 show poor structural stability in harsh conditions (water, acids, high temperatures), restricting use in complex matrices like industrial wastewater.[25,26] Pristine MOFs such as UiO-66 have limited functionality, requiring post-synthetic modifications (*e.g.*, nanoparticle loading) to enhance performance, increasing synthesis complexity and costs.[27] ZIF-8, with fixed micropores, is restricted to specific-sized molecules, limiting selective recognition of multi-component pollutants.[28] Noble metal-based MOFs (*e.g.*, Zr-based PCN-222, Ti-based MIL-125(Ti)) offer superior stability and activity but are costly for large-scale use.[29,30] Iron-based MOFs, by contrast, emerge as promising alternatives due to low cost, environmental friendliness, and enhanced structural robustness, making them well-suited to address limitations of conventional water treatment technologies.

Sai Zhang

Sai Zhang, member of the Communist Party of China, doctoral student, associate professor, graduated from Northwest University in 2018. Her main research direction is electrochemical sensing. In recent years, she has presided over 1 National Natural Science Foundation project and several provincial projects. She published 11 SCI papers during this period.

Yuping Tang

Yu-Ping Tang, PhD, is a Professor of Chemistry and PhD supervisor. His research focuses on complex substances in traditional Chinese medicine (TCM) and interactions between TCM and their components. He has presided over 10 national/provincial projects, including the National Key R&D Program and NSFC projects. As first/corresponding author, he has published over 300 papers, with 180+ indexed in SCI. His highest single-paper impact factor is 45.661.

As a type of MOF, Fe-MOFs have attracted significant attention due to their low toxicity, low cost, and mild synthesis conditions.[31] Among Fe-MOFs, the MIL series has become a research hotspot.[32] However, different members exhibit distinct properties: MIL-101(Cr) possesses a large specific surface area[33] but suffers from the toxicity of Cr sources and a large pore size,[34] which leads to poor selectivity for small molecules. MIL-53(Fe) exhibits a "breathing effect," which affects the repeatability of detection.[35] MIL-100(Fe) demonstrates strong acid resistance but shows a slow response,[36] making it unsuitable for rapid detection applications. In contrast, MIL-88 exhibits several advantages: it inherits the low cost and low toxicity characteristics of Fe-MOFs. It is constructed through the reaction of fumaric acid with Fe(III), forming a rigid three-dimensional porous framework without the "breathing effect," ensuring structural stability.[37] Its morphology can be tuned by adjusting synthesis conditions, ranging from nanorods and nanospheres to microcrystals. Scanning electron microscopy (SEM) and transmission electron microscopy (TEM) are commonly used to study its morphology.[38–40] This enables it to accommodate pollutants of varying sizes, significantly outperforming the fixed structure of MIL-101(Cr). Furthermore, MIL-88 exhibits superior thermal stability compared to MIL-100(Fe) and can be reused. Notably, in environmental applications, its reversible structural transformation, high adsorption capacity, and catalytic activity render it an ideal candidate for the detection and removal of emerging pollutants.[41–43]

While existing studies have explored the potential of MIL-88 as a functional material in the detection and removal of toxic pollutants, a systematic and in-depth evaluation of its synthetic strategies and environmental remediation applications remains lacking. Therefore, there is an urgent need for a timely and comprehensive review that integrates and analyzes the current findings to clarify their practical value in environmental science and guide future research directions. This review aims to fill this research gap by systematically summarizing the synthesis methods of MIL-88 and its applications in environmental fields, thereby promoting the development of such materials. As shown in Fig. 1, the synthesis and applications of MIL-88. In addition, this paper critically analyzes the challenges and limitations present in current research and explores its potential for sustainable environmental protection. Through this review, we hope to provide valuable insights into the design and application of MIL-88-based materials and to inspire further research and technological development in this field.

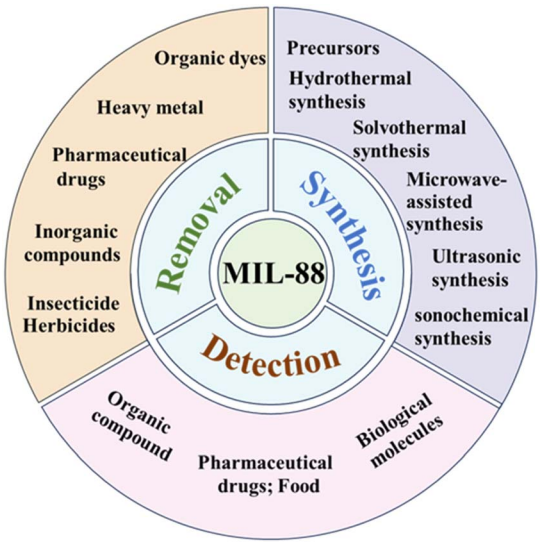

Fig. 1 An overview of the synthesis methods, detection, and the removal of contaminants using the metal–organic framework MIL-88 has shown significant efficiency.

2 Synthesis methods of MIL-88

2.1 Precursors

The MIL-88(Fe) is typically synthesized using $FeCl_3 \cdot 6H_2O$ and terephthalic acid as main precursors.[44] In 2006, Surblé *et al.* pioneered the synthesis of MIL-88, an MOF within the isoreticular family, using a controlled secondary building unit (SBU) approach.[45] This foundational work supported structural characterization *via* simulation methods. As shown in Table 1, iron(III) salts such as $FeCl_3 \cdot 6H_2O$ and $Fe(NO_3)_3 \cdot 9H_2O$ are commonly used as iron sources,[46] and the molar ratio of iron source to terephthalic acid is typically 1 : 1, as noted in previous studies.[47,48] Importantly, the morphology and size of MIL-88 can be controlled by adjusting reaction conditions (*e.g.*, solvent type, temperature, or additive concentration), which in turn enables the detection of pollutants with different sizes. Solvents are crucial for synthesis, affecting reaction kinetics and product properties. Dimethylformamide (DMF), ethanol, and water are often used, either alone or in mixtures.[31] While DMF is effective, its toxicity limits its use. Ethanol and water are more environmentally friendly but may hinder precursor solubility, impacting yield and quality.[37] Researchers have explored greener solvents or additives to optimize synthesis conditions and tailor MIL-88 properties.

To address limitations of traditional methods, innovative approaches have emerged. Microwave-assisted synthesis reduces reaction time and energy usage, while, mechanistically, the synthesis avoids the use of solvents, providing a sustainable alternative. Modulators or structure-directing agents have also been studied to enhance crystallinity and porosity, improving MIL-88's performance in environmental applications. These advances aim to mitigate issues like long reaction times, high energy consumption, and environmental concerns tied to conventional methods.

2.2 Hydrothermal synthesis

Hydrothermal synthesis is a widely used method for preparing MIL-88. This process involves mixing precursors in a solvent and transferring the mixture to a Teflon-lined autoclave. Reactions are typically conducted at 100–200 °C under autogenous pressure, with durations ranging from hours to days, depending on the target product properties and conditions.[67] Higher temperatures can accelerate reactions and influence crystal growth, but may lead to product decomposition if excessively

Table 1 Synthesis of MIL-88: precursors, process, morphology, size

Fe^{3+}/NH_2-BDC molar ratio	Solvent or mixed solvent	Process condition	Morphology	Size	Ref.
1 : 1	DMF 15 mL	Teflon-lined autoclave at 120 °C for 24 h	Regular spindles	Average size of approximately 1 μm	49
1 : 1	DMF and acetic acid (30 : 1)	Oil bath at 120 °C for 4 h	Regular octahedral figure	Average diameter of 100 nm	50
1 : 1	DMF 10 mL	Teflon-lined autoclave at 120 °C for 20 h	Diamond-like shape	Small particle size, and soft surface	51
1 : 1	DMF and NaOH (30 : 2)	Stainless steel autoclave at 100 °C for 12 h	Elongated hexagonal bipyramid	Average size of approximately 1 μm	44
1 : 1	CH_3OH, H_2O (4.5 : 1) dissolved in DMF	Ultrasound (150 W) at 120 °C for 2 h	Prismatic central portion (body) and pyramidal end portions (tips)	2.6 μm long × 0.5 μm wide	52
1 : 1	DMF 30 mL	Teflon-lined stainless autoclave at 120 °C for 24 h	Nanooctahedral crystals	Uniform size of ∼500 nm	53
1 : 1	Ultrapure water 25 mL	Teflon-lined stainless autoclave at 65 °C for 12 h	Hexagonal microrods	1 μm long and under 400 nm in diameter	40
1 : 1	DMF 30 mL	Teflon-lined autoclave at 120 °C for 20 h	Typical octahedral morphology	Average edge length of around 233 nm	54
1 : 1	DMF 15 mL	Stainless steel autoclave at 110 °C for 24 h	Sharp-ended rod-like prism-like structure	Size of approximately 0.5–3 μm	55
1 : 1	Deionized water 100 mL	Flask in oil bath at 100 °C for 4 h	Uniform polygonal-like nanostructure	Size of around 3.7 μm	56
1 : 1	DMF 15 mL	Round-bottom flask, at 120 °C, in an oil, under magnetic stirring for 3 h	Spindle-like structures, rod-type morphology	Average diameter of ∼180 nm	57
1 : 2	Deionized water 10 mL	Teflon-lined stainless autoclave in oven at 70 °C for 12 h	Octahedral structure	Lengths of 0.5–0.7 μm	58
1 : 1	DMF 50 mL	Teflon-lined autoclave at 120 °C for 20 h	Rod-like configuration and a core prism leading to hexagonal	Typical size of nearly 81.3 nm	59
0.3 : 1	DMF 10 mL, NaOH 2 mL	Autoclave at 100 °C for 15 h	Pyramidal structures	Typical size of nearly 81.3 nm	60
2 : 1	DMF 30 mL	Teflon-lined autoclave at 373 K (100 °C) for 20 h	Hexagonal pyramidal structures	The average size of approximately 1 μm	61
1 : 1	H_2O 10 mL	Autoclave at 65 °C for 18 h	Cubic bipyramidal hexagonal	Typical size of nearly 200 nm	62
1 : 1	DMF 50 mL	Round-bottom flask at 120 °C under reflux conditions for 12 h	Prism crystalline	Average size of approximately 2 μm	63
1 : 1	Deionized water 15 mL	80 mL solvent at 110 °C for 1440 min (24 h)	Regularly structured nanorods	Dimensions of approximately 500 nm	64
1 : 1	DMF 50 mL	Microwave oven (140 W) at 150 °C for 15 min	Spindle-like structures	Particle sizes 12.5 nm	65
1 : 1	DMF 15 mL	Teflon-lined autoclave at 185 °C for 2 h	Rod-like morphology with clear and distinct elongated structures	Dimensions of approximately 500 nm	66

high. The reaction pH also plays a critical role, as it affects metal ion coordination and organic linker deprotonation, ultimately impacting MIL-88 formation.[68]

Recent studies have further optimized the synthesis of MIL-88 and its derivatives. For instance, Lu *et al.* synthesized a novel layered multi-space composite material using a solvothermal method based on spindle-shaped FeCo-MIL-88 sulfide, nickel sulfide, and nickel oxide.[69] The composite was thermally treated at 350 °C under N_2 for 2 h with a ramping rate of 3 °C min^{-1} to enhance its structural stability and remove impurities. The resulting lamellar structure provided ample space for efficient electron transfer, leading to remarkable electrochemical properties. Specifically, the composite demonstrated an excellent specific capacitance and significant cycling stability, retaining 62.5% of its specific capacitance after 5000 cycles. Similarly, as shown in Fig. 2, Azari *et al.* synthesized a MIL-88A(Fe)/C composite *via* a hydrothermal process, combining MIL-88A with carbon. In addition, it combines the electro-Fenton process to degrade and treat the organic pollutants in dairy wastewater.[70] The composite's morphology and structure were characterized using spectroscopy and microscopy. Key parameters, including pH, reaction time, catalyst concentration, and oxidizer concentration, were optimized using response surface methodology (RSM). Optimal conditions for chemical oxygen demand (COD) reduction in the electro-Fenton process were pH 7.0, 102.6 min contact time, 0.5 g L^{-1} MIL-88A(Fe)/C, and 0.026 M $Na_2S_2O_8$. These results highlight MIL-88A(Fe)/C as an efficient catalyst for advanced wastewater treatment. In another

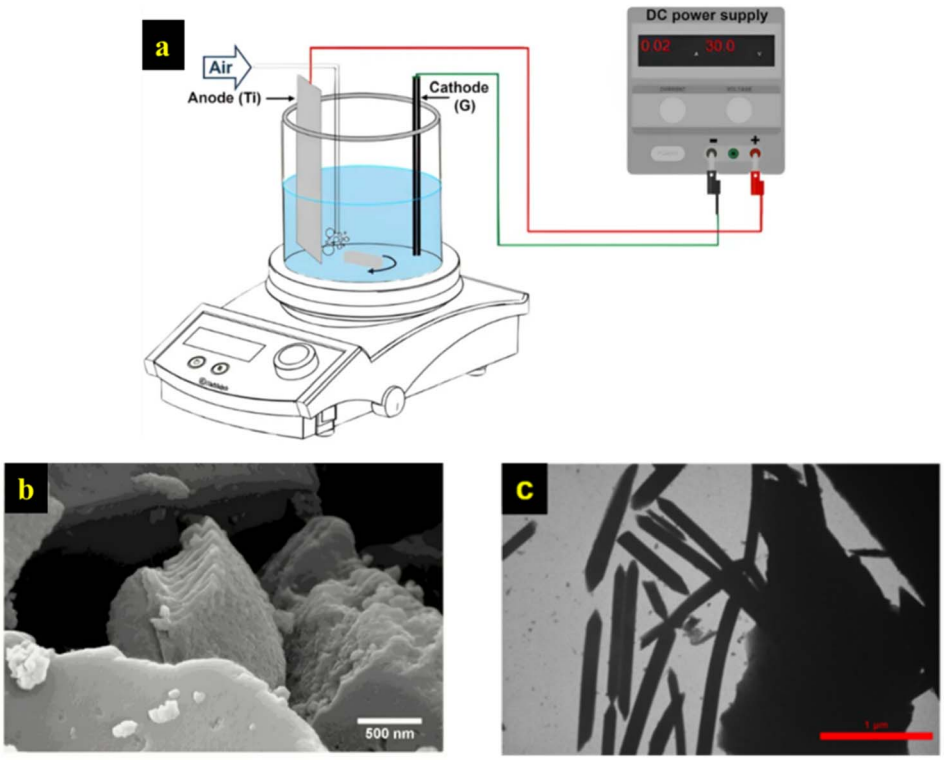

Fig. 2 The schematic view of the electro-Fenton system (a). SEM of MIL-88A(Fe) (b). TEM images of MIL-88A(Fe)/C (c). Reprinted with permission from ref. 70. Copyright (2025), *Sci. Rep.*

study, Guo *et al.* innovatively utilized the metal–organic framework (MOF) NH_2-MIL-88(Fe) as a precursor, introducing Ni doping to prepare a series of Fe_xNi_y-MOF materials and their bimetallic carbon derivatives (Fe_xNi_y/C) through solvothermal synthesis followed by high-temperature carbonization.[71] The results demonstrated that $FeNi_2$/C exhibited exceptional performance in the oxygen evolution reaction (OER), highlighting its potential as an efficient electrocatalyst for energy conversion applications.

2.3 Solvothermal synthesis

Solvothermal synthesis, similar to hydrothermal synthesis, employs organic solvents under reflux conditions instead of high-pressure autoclaves. By heating the reaction mixture below the solvent's boiling point, precise control over reaction conditions is achieved. Compared to hydrothermal methods, solvothermal synthesis often yields MIL-88 materials with unique properties. Key factors such as solvent type, reflux time, and temperature can be adjusted to control morphology, size, and functionality.[72] The choice of solvent significantly impacts precursor solubility and reaction kinetics, influencing product quality and yield. Additionally, solvothermal synthesis can reduce structural defects during crystal growth, enabling better control over morphology, pore structure, and functionalization. Beyond MOFs, solvothermal methods are effective for producing micro/nano carbons (M/NCs), such as carbon spheres, dots, and nanotubes, due to their low-temperature operation, environmental friendliness, and high yields.[73]

Recent studies highlight the versatility of solvothermal synthesis in creating MIL-88 materials for diverse applications. For example, in recent years, Han *et al.* used this method to fabricate a superhydrophobic wood surface by growing shuttle-like MIL-88(Fe) and incorporating an OPA reagent.[74] In 2019, Liao *et al.* demonstrated that the morphology of MIL-88A-Fe significantly influences its Fenton-like performance.[75] By varying the solvent ratio during solvothermal synthesis, they produced rod-like, spindle-like, and diamond-like MIL-88A-Fe.

Rod-like MIL-88A, with 60% exposed (100) facets, exhibited exceptional Fenton-like activity, achieving 100% phenol removal within 15 minutes at room temperature in the presence of H_2O_2. These findings underscore the critical role of morphology control in optimizing the catalytic performance of MIL-88A-Fe for environmental applications. In summary, solvothermal synthesis provides a flexible and efficient approach to tailor the properties of MIL-88 materials. Optimizing synthesis conditions enables the design of customized materials for applications such as energy storage and environmental remediation. Recent advancements underscore its potential for producing advanced, high-performance, and sustainable materials.

2.4 Microwave-assisted synthesis

Microwave-assisted synthesis has become a fast and effective way to prepare MOFs, including MIL-88. Using microwaves, the reaction temperature can quickly increase through dielectric heating, greatly reducing the reaction time compared to

traditional heating methods. In typical microwave-assisted synthesis, precursors and solvents are placed in a microwave reactor, and the reaction is carried out under controlled microwave power and time settings. For example, some studies have shown that applying microwave irradiation for just a few minutes to tens of minutes can produce MIL-88 with good crystallinity.[76] However, it's important to carefully control the microwave power and reaction time to avoid overheating or uneven heating, which could lead to defective or degraded materials.

In recent years, systematic research on microwave-assisted synthesis has been conducted. For instance, Arenas-Vivo *et al.* employed a comprehensive synthetic approach, utilizing microwave-assisted hydro/solvothermal reactions to systematically investigate the influence of various reaction parameters-such as reaction time, temperature, concentration, and solvent type, on the formation of well-established metal–organic frameworks (MOFs), including MIL-53-NH_2, MIL-88B-NH_2, and MIL-101-NH_2.[77] Similarly, in 2022, Zorainy *et al.* synthesized MIL-88B using a rapid microwave-assisted solvothermal approach under high-power conditions (850 W).[78] This method produced an iron-based MOF with 29% oxygen and 24% iron content, showing unique properties as an oxygen-rich catalyst for energetic systems. Compared to MIL-88 synthesized *via* the solvothermal method, the MIL-88 prepared using the microwave-assisted method exhibited enhanced peroxidase-like catalytic activity towards hydrogen peroxide.[79] The molecular weight-based method demonstrated significant advantages, including operational simplicity, rapid crystallization kinetics, excellent phase selectivity, and high product yield. These findings provide valuable insights into the catalytic mechanisms of MOFs, which will facilitate their practical application as artificial enzyme mimics.[80–82]

2.5 Ultrasonic and sonochemical synthesis

The ultrasonic method offers a quick, easy, and eco-friendly way for organic synthesis, particularly for creating MOFs. It uses cavitation bubbles to accelerate reactions and open new pathways, improving efficiency while addressing issues like long reaction times and high solvent use in traditional methods.[83,84] For example, Amaro-Gahete *et al.* showed that ultrasound-assisted synthesis of MIL-88A produces highly crystalline particles, which work well for ethylene adsorption.[52] Similarly, Abbasian *et al.* used ultrasound to grow MIL-88(Fe) inside magnetic polysaccharides (St/Fe_3O_4), forming St/Fe_3O_4/MIL-88(Fe) nanocomposites.[84]

Compared with the ultrasonic synthesis method, sonochemical synthesis utilizes ultrasonic waves to induce chemical reactions. In the synthesis of MIL-88, ultrasonic irradiation can promote the mixing of the precursors and enhance the mass transfer rate, which is conducive to the formation of the metal–organic framework. During the sonochemical process, cavitation bubbles are generated in the liquid phase, and the collapse of these bubbles generates high temperatures and pressures locally, which can accelerate the reaction. Some researchers have found that sonochemical synthesis can lead to the formation of MIL-88 with smaller particle sizes and higher surface areas.[31] However, the energy consumption and the scale-up of the sonochemical synthesis process need to be further optimized. For example, Liu *et al.* studied a series of MOF materials with piezoelectric properties.[85] These materials were synthesized *via* the ultrasonic method and applied to the piezoelectric photocatalytic reduction of Cr(VI). Abdpour *et al.* synthesized nanoparticles of MIL-88B(Fe) in a functional ionic liquid (FIL) medium under ultrasonic conditions.[86]

3 Removal of pollutants

3.1 Organic dyes

As typical persistent organic pollutants, organic dyes are widely residual in industrial wastewater from textile, printing, and other sectors. They not only affect the photosynthesis of aquatic organisms by shading water bodies but also pose risks to ecosystems and human health due to their teratogenic and carcinogenic properties. Moreover, their strong chemical stability makes complete removal difficult *via* traditional biodegradation and chemical oxidation technologies, thus highlighting the urgent need for developing efficient treatment techniques. MIL-88, photocatalytic adsorption has emerged as a highly effective and cost-efficient technology for removing persistent organic pollutants (POPs) from contaminated water. Among the various materials explored, MIL-88 has garnered significant attention due to its exceptional adsorption and photocatalytic properties. For instance, Li *et al.* demonstrated that MIL-88 effectively adsorbed organic contaminants such as tris-(2-chloroisopropyl) phosphate (TCPP).[87] When combined with H_2O_2 and visible light, amino-functionalized MIL-88B (MIL-88B-NH_2) achieved nearly complete degradation of TCPP within 60 minutes, highlighting its potential for treating organophosphate flame retardants in water. Similarly, Wang *et al.* developed an electro-Fenton coupled membrane filtration system (EF-MF) for the efficient removal of bisphenol A (BPA), a common pharmaceutical and personal care product (PPCP).[88] The EF-MF system exhibited excellent removal efficiency and long-term stability, showcasing its practical applicability.

3.2 Heavy metal

Heavy metal pollution has emerged as one of the most pressing environmental issues today. The treatment of heavy metals is particularly challenging due to their environmental persistence and resistance to degradation. In recent years, numerous approaches for removing heavy metals from wastewater have been widely investigated.[89] To address this, Wang and colleagues modified MIL-88B(Fe) *in situ* with polyethylene glycol 4000 (PEG-4000) and ammonium phosphomolybdate hydrate (AMP), creating an effective adsorbent for Sr^{2+} removal.[90] In another study, Zango *et al.* found that MIL-88(Fe), NH_2-MIL-88(Fe), and mixed-MIL-88(Fe) removed anthracene (ANT) with efficiencies of 98.3%, 92.4%, and 95.8%, respectively, within just 25 minutes.[91] Ghazali *et al.* further demonstrated the versatility of MIL-88 by reporting that both UVA/MIL-88-A/PS and solar/MIL-88-A/PS systems effectively degraded

naphthalene (NAP), with the solar/MIL-88-A/PS system achieving complete degradation within 10–15 minutes.[92]

3.3 Inorganic compounds

Inorganic compounds incorporating transition metals—including palladium (Pd), nickel (Ni), manganese (Mn), iron (Fe), and copper (Cu)—find widespread application across industrial manufacturing and catalytic processes. Without adequate treatment, these compounds are prone to leaching into aquatic systems, where their environmental and health implications become pronounced. Notably, many of these transition metals exist in forms classified as heavy metals, exhibiting high toxicity; certain species are even recognized as carcinogens. Collectively, their presence in water sources poses substantial risks to ecological integrity and human well-being. As shown in Fig. 3, Huo *et al.* addressed this issue by developing a novel nanostructured material, MIL-88A-layered double hydroxides (LDHs), *via* a two-step solvothermal method.[93] The adsorption mechanism is achieved through the combined effects of CO_3^{2-} forming precipitates with Pb(II) and surface hydroxyl groups acting as adsorption sites. This material featured a chestnut-like unique structure and exhibited excellent removal performance towards Pb^{2+} from water in comparison to MIL-88A(Fe). Bakhtian *et al.* further advanced the field by synthesizing a double-shelled $NiCo_2O_4$@MOF-801@MIL88A ternary heterojunction, which exhibited exceptional photocatalytic performance for the degradation of both organic and inorganic pollutants.[94] Furthermore, the effects of drug concentrations, reaction pH, photocatalyst amount, scavenger type, and others have been investigated to achieve the optimized reactions and best response.

3.4 Pharmaceutical drugs

The persistent presence of emerging contaminants in aquatic environments remains a critical challenge, given that millions of individuals depend on unsafe water sources for daily use. Concomitant with the advancement of the pharmaceutical industry, aquatic systems are increasingly burdened by pharmaceutical residues.[95,96] Like organic dyes, most pharmaceuticals exhibit high chemical stability and are recalcitrant to degradation by biological processes such as phytoremediation.[97] Developing efficient adsorbents with appropriate pore sizes for the removal of pharmaceuticals poses significant challenges. The integration of MIL-88 with other materials has also shown remarkable results. This section will elaborate on recent advances in the application of MIL-88 for the treatment of doxycycline and diclofenac.

Doxycycline (DOX/cationic antibiotic drug) is the drug used in the treatment of this pandemic. These drugs are very toxic, and their discharge into water can cause side effects on human health. Thus, effective removal of these drugs from both drinking water and wastewater is crucial for public health.[98] For example, Karimi *et al.* prepared magnetic graphene oxide@MIL-88 alginate hydrogel beads, as shown in Fig. 4, which effectively removed COVID-19 drugs such as doxycycline (DOX), hydroxychloroquine (HCQ), naproxen (NAP), and dipyrone (DIP).[99] The authors demonstrated that the adsorption mechanism involved hydrogen bonding, π–π interactions, electrostatic interactions, hydrophilic interactions, and acid–base interactions. Furthermore, it was validated that the preparation of MIL-88 and its composites exhibited sustainability, cost-effectiveness, environmental friendliness, and excellent recyclability, making them suitable for practical applications such as wastewater treatment.

Diclofenac sodium, a non-steroidal anti-inflammatory drug (NSAID), is ubiquitously present and is frequently detected in the aquatic environment as a continual toxic waste and has been identified as a persistent harmful pollutant.[100] Recently, Hemkumar *et al.* synthesized Fe-based MOFs (MIL-88(Fe)) and created a ternary photocatalyst (MIL-88(Fe)/Ag_3PO_4/GCN, MAG) to enhance visible-light absorption and charge transfer efficiency, successfully degrading diclofenac (DCF) under simulated sunlight.[42] They observed that the uptake of diclofenac is predominantly dependent on pH, with optimal performance achieved at approximately pH 3. The degradation pathway was

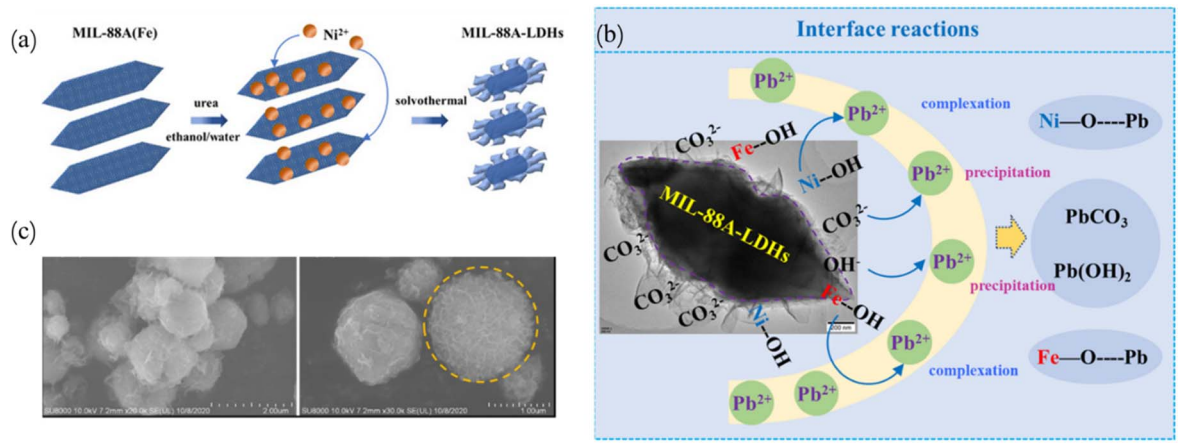

Fig. 3 Schematic illustration of the synthesis process of MIL-88A-LDHs (a). Schematic illustration of the mechanism of Pb^{2+} adsorption by MIL-88A-LDHs (b). SEM images of MIL-88A-LDHs (c). Reprinted with permission from ref. 93. Copyright (2022), MDPI.

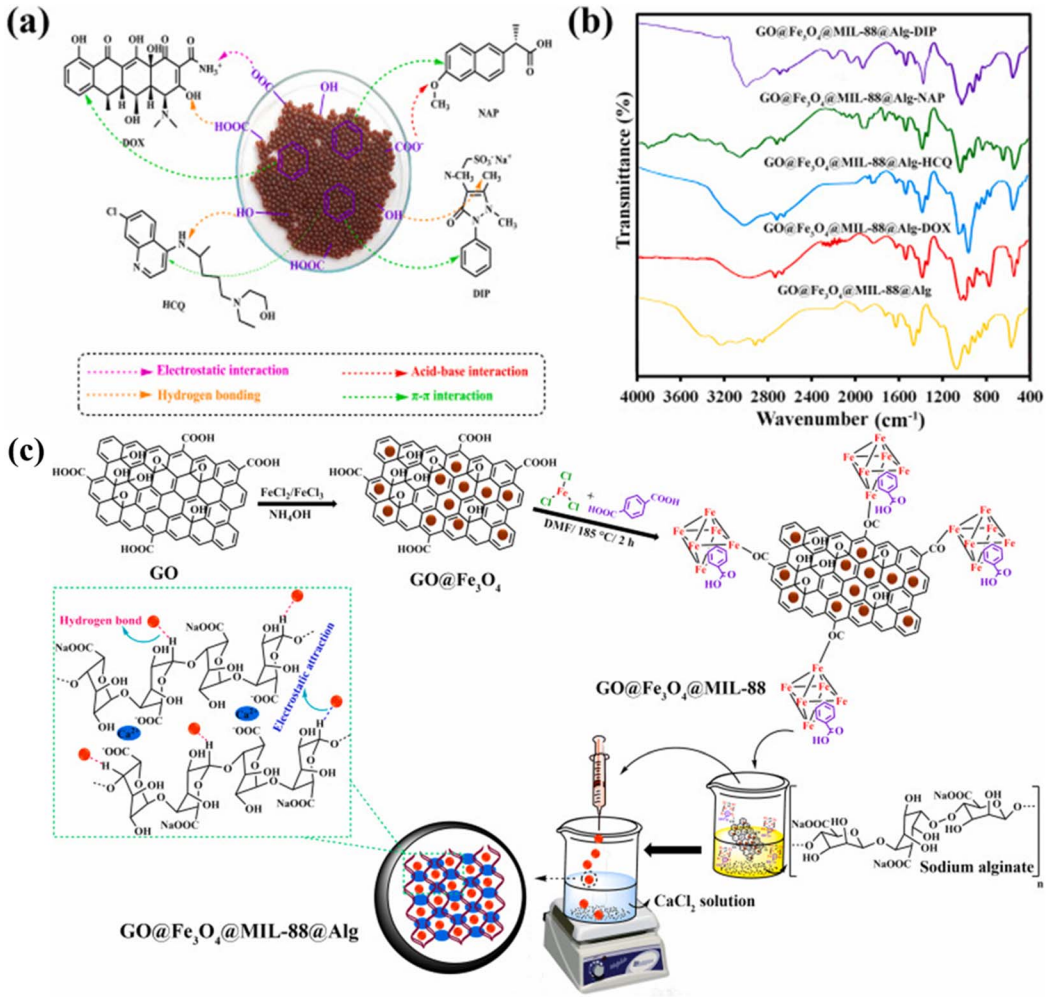

Fig. 4 Proposed adsorption mechanism of DOX, HCQ, NAP, and DIP onto GO@Fe_3O_4@MIL-88@Alg hydrogel beads. (a) FT-IR analyses of GO@Fe_3O_4@MIL-88@Alg hydrogel beads post-adsorption of DOX, HCQ, NAP, and DIP. (b) Schematic of sequential steps for removal of COVID-19 drugs using GO@Fe_3O_4@MIL-88@Alg hydrogel beads. (c) Reprinted with permission from ref. 99. Copyright (2024), Elsevier.

primarily achieved through hydroxyl radical attack and hydroxylation. This study proposes a novel approach that can be utilized in future research for synthesizing photocatalysts aimed at degrading pharmaceuticals in aqueous solutions.

3.5 Insecticides and herbicides

Insecticides, encompassing synthetic and biological agents, are specifically formulated to eradicate disease-transmitting insects, regulate insect pest populations, and alleviate insect-mediated plant infestations. MIL-88, known for their multi-functionality, chemical stability, and high surface area, are widely employed as adsorbents in water treatment processes to remove contaminants, thereby improving water quality and ecosystem health. Recent studies have also highlighted the potential of MIL-88 in adsorbing specific pollutants. As shown in Fig. 5, Alluhaybi *et al.* found that MIL-88(Fe)-NH_2 had a maximum adsorption capacity of 345.25 mg g^{-1} for 2,4-dichlorophenylacetic acid, surpassing previous adsorbents.[101] The study investigated the adsorption of atrazine and 2,4-dichlorophenylacetic acid using synthesized MIL-88(Fe)-NH_2. Adsorption occurred *via* hydrophobic, π–π interactions, and pore-filling processes. Under optimal conditions, the synthesized material exhibited a 2,4-dichlorophenylacetic acid removal capacity of 445.25 mg g^{-1}. Chiani *et al.* optimized the degradation of imidacloprid (IMC) using mesoporous NH_2-MIL-88B(Fe)/graphite carbon nitride nanocomposites, further demonstrating the versatility of MIL-88-based materials.[102] The findings suggest that MIL-88(Fe)-NH_2 is a cost-effective alternative for removing pollutants from aqueous solutions.

In summary, MIL-88 and its derivatives have proven to be highly effective in the photocatalytic adsorption and degradation of a wide range of pollutants, including organic contaminants, heavy metals, and pharmaceutical residues. By integrating MIL-88 with other functional materials and optimizing synthesis methods, researchers have developed innovative solutions for environmental remediation. These advancements underscore the potential of MIL-88-based technologies in addressing global water pollution challenges.

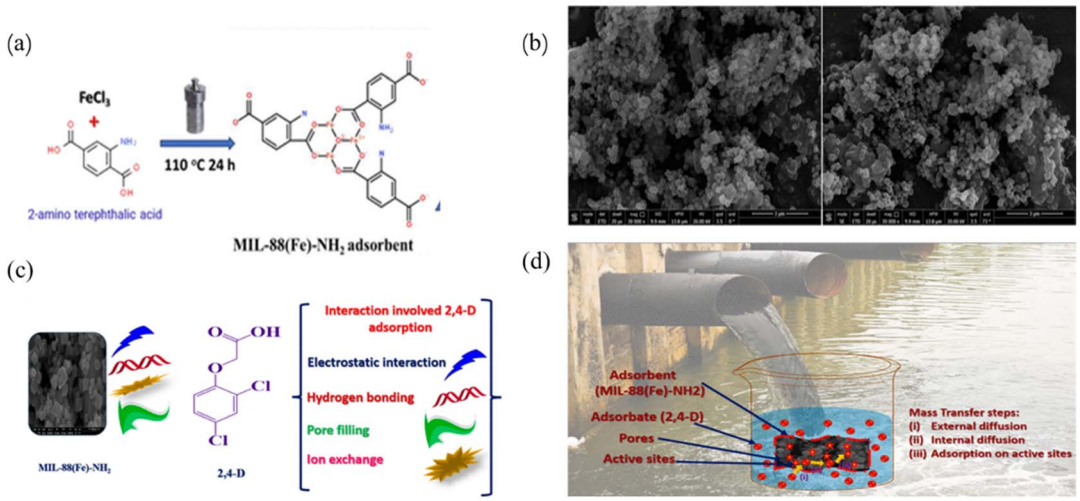

Fig. 5 Hydrothermal synthesis of MIL-88(Fe)-NH_2. (a) SEM images of MIL-88(Fe)-NH_2: before adsorption (left) and after five reuse cycles (right). (b) Interaction mechanism between MIL-88(Fe)-NH_2 adsorbent and 2,4-dichlorophenylacetic acid molecule. (c) Diffusion mechanism of 2,4-dichlorophenylacetic acid onto MIL-88(Fe)-NH_2. (d) Reprinted with permission from ref. 101. Copyright (2023), ACS.

4 Detection of pollutants

4.1 Potentials of MIL-88-based sensors

MIL-88 has emerged as a highly versatile material for detecting and addressing various pollutants, with applications spanning environmental monitoring, food safety, and biomedical fields. Its unique properties, such as high surface area, tunability, and functional adaptability, make it a valuable tool for tackling complex challenges. Compared to traditional methods such as gas chromatography-mass spectrometry (GC-MS) or high-performance liquid chromatography (HPLC), MIL-88-based materials offer distinct advantages: versatility, tunability, cost-effective preparation, and simplified testing processes.[103] For example, Ghorbani *et al.* synthesized melamine-modified MIL-88 *via* a solvothermal method and encapsulated it in a tea bag filter membrane to fabricate a μ-SPE device, which can efficiently extract VOCs (*e.g.*, BTEX) from water samples, highlighting its advantage in simplifying detection procedures.[104] Similarly, Wang *et al.* developed Fe-MIL-88-NH_2 combined with a d-SPE method for TBBPA extraction in water, and further integrated this system with HPLC for environmental monitoring, which confirms its feasibility in practical applications.[105,106]

MOF-based functionalized sensors (*e.g.*, such as chemiluminescence (CL), fluorescence (FL), electrochemiluminescence (ECL), and electrochemical sensors (EC)) have demonstrated strong capabilities in detecting hazardous exogenous pollutants, with MIL-88 and its composites standing out among them.[107] As shown in Table 2, compared with other MOF materials such as MIL-53, MIL-100, ZIF-8, and UiO-66, the advantages of MIL-88 and its composites are reflected in multiple aspects: In terms of detection targets, most other MOF materials are limited to single categories of pollutants or conventional biomolecules. In contrast, MIL-88 and its composites can cover diverse complex targets, including volatile organic compounds (VOCs), persistent organic pollutants (POPs), biomarkers, heavy metals, and pesticide residues. They have also expanded into the field of biomedical detection.[108] For example, Liu *et al.* developed NH_2-MIL-88 modified magnetic Nb_2CT_x, which can sensitively detect polychlorinated biphenyls (PCBs) in water *via* magnetic solid-phase extraction (SPE), effectively addressing the health risks posed by POPs.[109]

4.2 Organic compound

Recently, water pollution by organic pollutants such as dyes, phenols, pharmaceutical products, herbicides, insecticides, nitro-aromatic compounds, and other inorganic compounds like fluorides has increased due to the constant release of their effluents into aquatic media.[149] Accordingly, the detection of these compounds has attracted significant research interest, inspiring subsequent studies. In 2022, a fluorescence sensor based on NH_2-MIL-88(Fe)@Cu^{2+} was developed. By incorporating CTAB for self-assembly and forming microspheres, the MOF fluorescence sensor was attracted to 3-nitro-L-tyrosine (3-NT) through electrostatic forces. In comparison to other fluorescence methodologies, this sensor exhibited a lower detection limit (41.1 nM), negated the need for complex pre-treatment processes, and demonstrated minimal sensitivity to temperature fluctuations, providing results within 7 min post-sample addition.[114] Looking ahead, these research results establish a foundational basis for various applications and potential advancements in the expansive field of fluorescence sensing technology. In the same year, Ren *et al.* synthesized a novel electrode material, P-doped Fe/Fe_3O_4@C, by calcining MIL-88 at 700 °C and subsequently annealing it with NaH_2PO_2 for two hours.[150] This material demonstrated significantly improved detection sensitivity for 4-nitrophenol (4-NP), a prevalent organic pollutant in environmental samples. The superior sensing performance of P_{2h}-Fe/Fe_3O_4@C-700/GCE can be attributed to the incorporation of phosphorus, which enhances

Table 2 Detection performance of MIL-88(Fe), its composites, and other MOF materials in the treatment of emerging pollutants

MOF type	Target pollutants	Dose	Equilibrium time	pH	Linear range	Detection limit	Types of sensors	Ref.
NH_2-MIL-88	*Salmonella*	80 μg	360 s	Not reported	1.01×10^2 to 1.01×10^6 CFU mL^{-1}	93 CFU mL^{-1}	Immunosensor	110
NH_2-MIL-88	Maduramicin NT-proBNP	2 μg mL^{-1}	40 s	6.00	0.1–50 ng mL^{-1}	0.045 ng mL^{-1}	Immunosensor	111
MIL-88@1T-MoS_2	CD44	60 mg	2700 s	Not reported	1 fg mL^{-1} to 1 ng mL^{-1}	0.21 fg mL^{-1}	Immunosensor	112
MIL-88	3-Nitro-L-tyrosine	5.0 mg mL^{-1}	3600 s	7.00	0.5–500 ng mL^{-1}	1.4 pg mL^{-1}	Immunosensor	113
NH_2-MIL-88	Dopamine	0.02 mg mL^{-1}	420 s	8.80	0–30 μM	41.1 nM	Fluorescence sensor	114
MIL-88	Chloramphenicol	10 μg mL^{-1}	2100 s	5.40	50 nM to 30 μM	46 nM	Fluorescence sensor	115
NH_2-MIL-88	*Salmonella*	150 μg mL^{-1}	4500 s	Not reported	0.005–0.3 μM	0.028 μg L^{-1}	Fluorescence sensor	116
MIL-88@Pd/Pt	Arsenic	25 μg	480 s	Not reported	8.0×10^1 to 8.0×10^6 CFU mL^{-1}	35 CFU mL^{-1}	Colorimetric biosensor	117
NH_2-MIL-88	Glutathione	10.00 μg mL^{-1}	900 s	4.80	5.00–600.00 μg L^{-1}	2.78 μg L^{-1}	Colorimetric biosensor	118
MIL-88	Hydrogen peroxide	62.5 μg mL^{-1}	3600 s	3.00	0.55–3 μM	36.9 nM	Colorimetric biosensor	119
MIL-88B	Tetracycline	3 mg mL^{-1}	3000 s	4.50	10–100 μM	0.60 μM	Colorimetric biosensor	120
MIL-88	Cd^{2+}	3.33 mg mL^{-1}	1800 s	3.50	50–1000 nM	46.75 nM	Colorimetric biosensor	121
NH_2-MIL-88(Fe)-rGO	Pb^{2+}	1 mg mL^{-1}	240 s	5.17	0.05–0.75 μg L^{-1}	4.9 nM	Electrochemical sensor	122
NH_2-MIL-88(Fe)-rGO	Cu^{2+}	1 mg mL^{-1}	240 s	5.17	0.01–0.3 μM	3.6 nM	Electrochemical sensor	122
NH_2-MIL-88(Fe)-rGO	Malathion	1 mg mL^{-1}	240 s	5.17	0.005–0.05 μM	10 nM	Electrochemical sensor	122
CdTe QDs@NH_2-MIL-88	Carcinoembryonic antigen	1 μg L^{-1}	3600 s	7.40	1.0×10^{-6} to 1.0 μg L^{-1}	0.3 pg L^{-1}	Electrochemical sensor	123
MIL-88		10 nM	900 s	7.40	0.01–100 ng mL^{-1}	1.5×10^{-3} ng mL^{-1}	Electrochemical sensor	124
MIL-88A	Cholylglycine	1 mg mL^{-1}	15 s	7.00	0.01–50 nM	3.4 pM	Electrochemical sensor	125
MIL-88	Pathogenic bacteria	10^3 CFU mL^{-1}	900 s	6.50	$10–10^8$ CFU mL^{-1}	1 CFU mL^{-1}	Electrochemical sensor	126
MIL-88	Kojic acid	100 μM	Not reported	7.00	1.0 μM to 1.5 mM	0.73 μM	Electrochemical sensor	127
MIL-101(Cr)	Tartrazine	2 mg	180 s	2.0	0.004–0.1 μM	1.77 nM	Electrochemical sensor	128
MIL-101(Cr)-NH_2	Ammonia	500 ppm	8 s	Not reported	0.7–600 ppm	0.58 ppm	Gas sensor	129
MIL-53(Fe)	Flusilazole	0.100 nM	150 s	6.50	1.00×10^{-4} to 1.00×10^{-12} mol L^{-1}	593 fM	Electrochemical sensor	130
MIL-53(Fe)	Carcinoembryonic antigen	3 mg mL^{-1}	Not reported	7.50	10^{-5} to 10 ng mL^{-1}	4.04 fg mL^{-1}	Immunosensor	131
MIL-100(Fe)	TPTH	4 mg L^{-1}	60 s	11.00	10–1000 μg L^{-1}	210 ng L^{-1}	Chemiluminescence (CL) sensor	132
Pt/Au MIL-100(Fe)	Deoxynivalenol	100 ng mL^{-1}	Not reported	6.50	50–5000 ng mL^{-1}	44.14 ng mL^{-1}	Colorimetric aptasensor	133
MIL-125(Ti)	Fenitrothion	0.96 nM	480 s	7.50	1–9000 nM	0.96 nM	Electrochemical sensor	134
MIL-125(Ti)/TiO_2	Formaldehyde	450 ppb	37 s	Not reported	25–1000 ppb	4.51 ppb	Gas sensor	135
ZIF-8/MoO_3	H_2S	80 ppm	20 s	Not reported	1–100 ppm	12.86 ppb	Gas sensors	136
UiO-66(Zr)	Methyl parathion	1 μM	80 s	7.00	0.01–10 μM	8.05 nM	Electrochemical sensor	137
	Methylmercury	500 ppb	360 s	4.50	100–500 ppb	0.317 ppb	Electrochemical sensor	138
Mn_3O_4-UiO-67	Arsenic(III)	5 μM	250 s	Not reported	2.7–40 nM	0.42 nM	Electrochemical sensor	139
GO/UiO-67@PtNPs	Ciprofloxacin	10 μmol L^{-1}	Not reported	7.00	0.05–180 μmol L^{-1}	0.0026 μmol L^{-1}	Electrochemical sensor	140
	Ochratoxin A	5.0 μM	Not reported	7.40			Electrochemical sensor	141

Table 2 (*Contd.*)

MOF type	Target pollutants	Dose	Equilibrium time	pH	Linear range	Detection limit	Types of sensors	Ref.
HKUST-1/ $CoFe_2O_4$/g-C_3N_4					1.0×10^{-2} to 100.0 ng mL^{-1}	4.3×10^{-3} ng mL^{-1}		
Hemin@HKUST-1	Chloramphenicol	0.05 ng mL^{-1}	1800 s	7.40	0.15–100 ng mL^{-1}	0.0138 ng mL^{-1}	Electrochemical sensor	142
PCN-222	4-Nonylphenol	5.0 μM	360 s	8.00	$1 \times 10^{-4} \times 10$ μM	0.03 nM	Electrochemical sensor	143
PCN-222@MIPIL	CO_2	2000 ppm	75 s	Not reported	66.89–2000 ppm	Not reported	Gas sensor	144
MOF-74								
Cu-MOF-74	Aromatic vapors	Not reported	20 s	Not reported	0.1–100 ppm	68 ppb	Gas sensor	145
MOF-808	Nitrofurazone	100 μM	Not reported	Not reported	Not reported	0.51 μM	Fluorescent sensor	146
Ce-MOF-808@CeO_2	Antibiotic tetracycline	100 nM	2100 s	Not reported	1 pM to 100 nM	0.21 pM	Electrochemical sensor	147
Au@MOF-303	Humidity	3.39% RH	14 s	Not reported	4345 Hz to 3.39% RH	0.18% RH	Low-humidity sensors	148

electron transfer efficiency and introduces additional active sites. These characteristics provide new insights for advancing research in the sensing field.

4.3 Food detection

Food safety remains a critical concern in the food industry, involving issues such as contamination, excessive additive use, nutritional supplementation, and preservation practices. Thus, rapid detection methods are critical for effective food safety surveillance. Ochratoxin A (OTA), a toxic secondary metabolite produced by *Aspergillus* and *Penicillium* fungi under natural conditions, poses severe contamination risks to agricultural products and fermented foods.[151] In a recent study, Yu *et al.*[152] computationally designed a high-affinity molecular recognition peptide targeting OTA *via* structural analysis and molecular dynamics simulations. A novel fluorescent probe, RhB-MRP (MRP-lysine-rhodamine B) (Fig. 6), was subsequently synthesized. Using this RhB-MRP probe, a ratiometric fluorescence biosensor was constructed by integrating the classical blue-fluorescent metal–organic framework (MOF), NH_2-MIL-88(Fe). This biosensor demonstrates advantages, including a low detection limit and high sensitivity. Such advancements further expand the potential applications of peptides in recognition technologies. Additionally, Fan *et al.* constructed a "turn-on" fluorescent sensor, CeO_2@MIL-88B, for detecting thiabendazole (TBZ) with a remarkably low detection limit of 0.294 μm and excellent selectivity.[153] For foodborne pathogens, a microfluidic biosensor was developed to detect *Salmonella*, achieving rapid detection at concentrations as low as 35 CFU mL^{-1}, further underscoring MIL-88's applicability in ensuring food safety.[117]

4.4 Pharmaceutical drugs detection

Many drugs are used as feed additives to help livestock resist disease, boost immunity, and promote growth. However, long-term use may not only be ineffective but also pose potential health risks to humans through the consumption of dairy products, as drugs can transfer from feed to milk. Additionally, the combination of drugs with MOFs for drug delivery highlights the importance of effective drug detection.[154] For example, Chiñas-Rojas *et al.* explored MOF–drug interactions, emphasizing their potential in targeted drug delivery systems, particularly for cancer therapy.[155] Similarly, Salandari-Jolge *et al.* developed an aptasensor for insulin detection, demonstrating high sensitivity and selectivity, which could revolutionize diabetes management.[156] As shown in Fig. 7, Darvishi *et al.* in this work is to synthesize a novel carrier system *via* the coordination of MIL-88(Fe) with carboxymethyl cellulose (CMC), aiming to enhance drug–carrier interactions.[157] Notably, the tetracycline (TC)-loaded carrier exhibits *in vitro* cytocompatibility with human skin fibroblast cell lines and significant antibacterial activity against both *Escherichia coli* (*E. coli*) and *Staphylococcus aureus* (*S. aureus*). In electrochemical sensing, Wang *et al.* utilized Fe-MIL-88/CP for the simultaneous detection of dopamine and ascorbic acid, achieving high sensitivity and low detection limits.[158] Therefore, NH_2-MIL-88(Fe) represents a promising carrier for the localized delivery of drugs to various tissues to improve drug absorption.

4.5 Biological molecules detection

The intrinsic peroxidase-like activity of MIL-88 has also been exploited for biomolecule detection. Zhao *et al.* utilized MIL-88(Fe) for colorimetric detection of glucose and biothiols,[115] while Gao *et al.* confirmed its peroxidase-like activity, which accelerated the oxidation of TMB in the presence of H_2O_2.[159] Extending these applications, Jiang *et al.* prepared bimetallic MIL-88(NH_2) for the sensitive detection of extracellular vesicles (EVs), coupling it with glucose oxidase (GOx) to enhance sensitivity, highlighting its potential in biomedical research and diagnostics.[160] From environmental monitoring to food safety, drug delivery, and biomolecule detection, MIL-88 has demonstrated remarkable versatility and effectiveness. Its

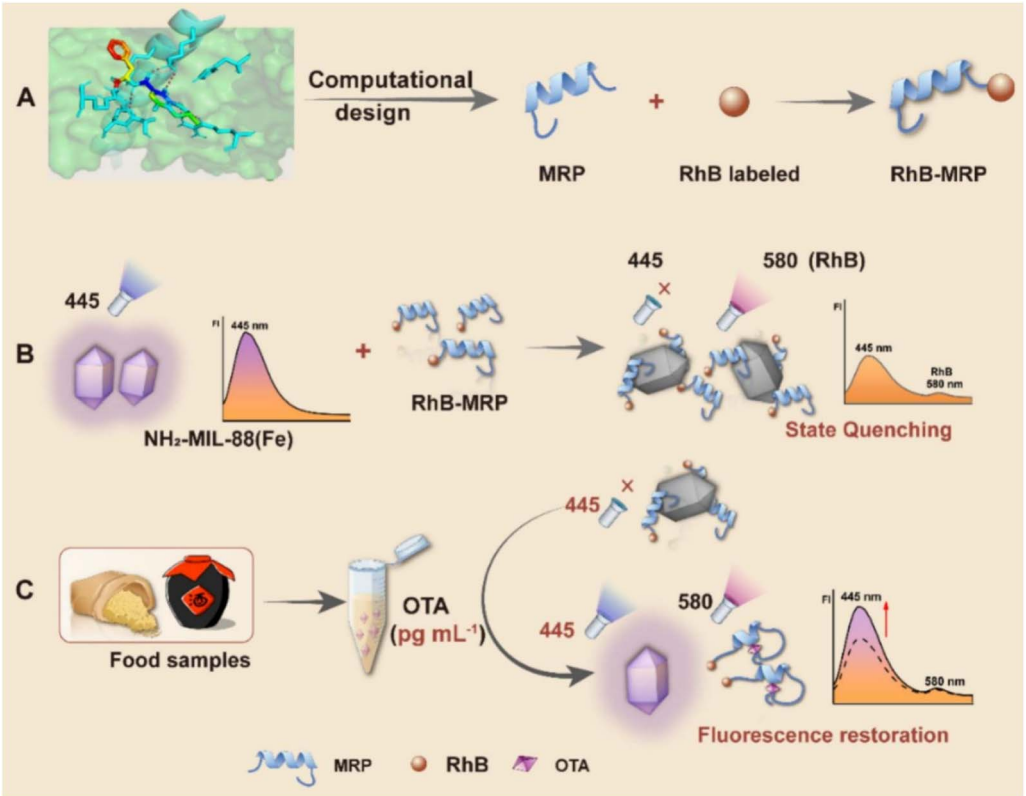

Fig. 6 Schematic diagram for the construction of fluorescence biosensor based on RhB-MRP and NH_2-MIL-88(Fe). (A) Design of MRP and Pep-RhB. (B) Synthesis of NH_2-MIL-88(Fe) and its fluorescence quenching upon interaction with RhB-MRP. (C) Fluorescence recovery of NH_2-MIL-88(Fe) upon addition of OTA. Reprinted with permission from ref. 152. Copyright (2025), Elsevier.

ability to be functionalized and integrated with other materials has opened new avenues for addressing complex challenges in environmental science, healthcare, and analytical chemistry. As research continues to advance, MIL-88-based technologies are poised to play an increasingly important role in ensuring environmental sustainability, public health, and food safety. Future studies should focus on scaling up these applications and exploring their potential in real-world scenarios to fully realize their transformative impact.

5 Challenges and prospects

MIL-88, a subclass of metal–organic frameworks (MOFs), has garnered significant interest owing to its high porosity and structural flexibility. While it shows promise in applications such as gas storage, drug delivery, and catalysis, its potential as a pollutant detection platform remains underexplored. Specifically, its full capabilities in detecting hazardous substances—including heavy metals, pharmaceuticals, and endocrine-disrupting compounds—have yet to be fully realized. Currently, MIL-88(Fe)-based sensors suffer from insufficient sensitivity and selectivity toward trace pollutants in complex matrices, which limits their practical deployment in real-world environmental monitoring and early warning systems. Additionally, the environmental impact of post-treated MIL-88(Fe) remains unclear, with potential secondary pollution risks arising from the lack of sustainable post-treatment protocols.

To address these limitations, future research should focus on three key areas: first, expand the application scope of MIL-88(Fe) to cover emerging pollutants such as microplastics and endocrine disruptors. Second, enhance detection performance by integrating MIL-88(Fe) with advanced sensing technologies (*e.g.*, plasmonic sensors or electrochemical platforms). Third, improve scalability and sustainability through green synthesis routes—such as solvent-free methods or the use of renewable resources—and conduct field trials in real-world settings (*e.g.*, wastewater treatment plants) to validate practical feasibility. Notably, several knowledge gaps must be addressed to support these advancements. Although MIL-88 synthesis and its pollutant removal/detection capabilities have been reported, the precise mechanisms governing its structural flexibility and responsiveness to external stimuli (*e.g.*, temperature, pressure, or guest molecules) remain incompletely understood. Furthermore, its long-term stability and degradation pathways under practical conditions—particularly in aqueous or biological environments—require further investigation. To fill these gaps, priority should be given to optimizing synthesis methods for scalability and reproducibility, exploring their potential in emerging fields (*e.g.*, environmental remediation, energy storage, and biomedicine), and applying advanced characterization techniques (*e.g.*, *in situ* spectroscopy and computational

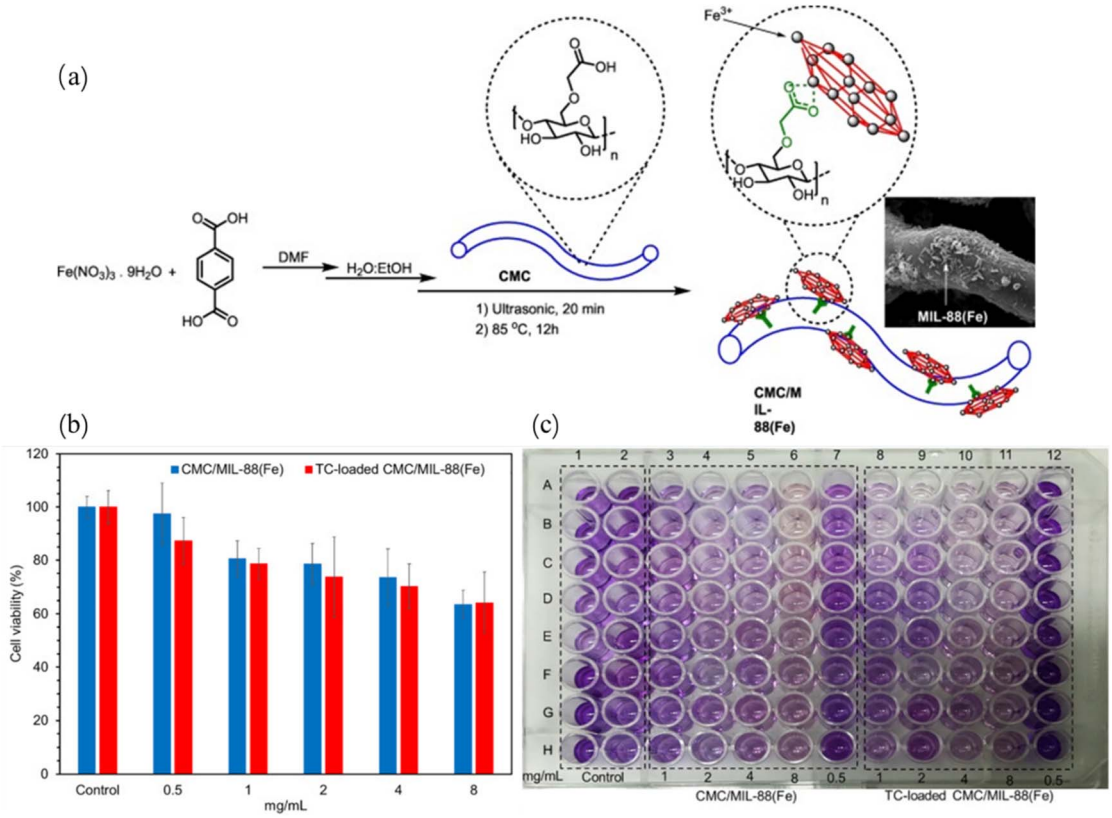

Fig. 7 *In situ* formation of MIL-88(Fe) in the presence of CMC fibers for constructing CMC/MIL-88(Fe) composites, with the SEM image of the product. (a) Cell viability (%) of human skin fibroblast HFF-1 cells after 48 h incubation with various concentrations of CMC/MIL-88(Fe) and TC-loaded CMC/MIL-88(Fe), along with corresponding cell growth images (data presented as mean ± SD, $n = 8$) (b and c). Reprinted with permission from ref. 157. Copyright (2021), Elsevier.

modeling) to elucidate dynamic behaviors and molecular interactions. Resolving these issues is critical to unlocking the full potential of MIL-88 in both academic research and industrial applications.

6 Conclusions

This paper presents a systematic review of the synthesis and applications of MIL-88. At the synthesis level, it comparatively analyzes the effects of different synthesis conditions (such as solvothermal method, microwave-assisted method, *etc.*) on material properties, and clarifies the advantages and applicable scenarios of each method. In terms of material characteristics, MIL-88 has a unique crystal structure, appropriate porosity, regular morphology, and high crystallinity, which lays a foundation for its interaction with pollutants. In terms of applications, compared with other MOF materials, MIL-88-based sensors exhibit more excellent sensitivity in detecting pollutants such as organic dyes, heavy metals, and pharmaceuticals; their adsorbents also show significant advantages in removing various pollutants due to their high adsorption capacity. Moreover, the synergistic effect of adsorption and catalytic degradation further improves the efficiency of pollutant treatment. However, there are still some literature gaps in current research, such as insufficient research on its long-term stability and unclear interface interaction mechanism after compounding with other materials. Future research can focus on optimizing the synthesis process to reduce costs, expanding modification methods to enhance performance, and deepening the integration with other technologies, so as to promote the practical transformation of MIL-88 in the environmental field and provide more powerful material support for the development of pollutant remediation and sensing technologies.

Data availability

No primary research results, software or code have been included, and no new data were generated or analysed as part of this review.

Conflicts of interest

The authors declare that they have no known competing financial interests or personal relationships that could have appeared to influence the work reported in this paper.

Acknowledgements

The authors gratefully acknowledge financial support from the National Natural Science Foundation of China (82304685), the

Natural Science Foundation of Shaanxi Province (2023-YBSF-245). Sanqin Talent Special Support Program Innovation and Entrepreneurship Team Project (2023). Xianyang Chinese Medicine Industrial Innovation Cluster Project of Qin Innovation Source (L2024-QCY-ZYYJJQ-X51).

Notes and references

1 V. Kumar, E. Singh, S. Singh, A. Pandey and P. C. Bhargava, *Chem. Eng. J.*, 2023, **459**, 141568.
2 B. S. Rathi, P. S. Kumar and D.-V. N. Vo, *Sci. Total Environ.*, 2021, **797**, 149134.
3 Y.-G. Chen, J.-H. Huang, R. Luo, H.-Z. Ge, A. Wołowicz, M. Wawrzkiewicz, A. Gładysz-Płaska, B. Li, Q.-X. Yu and D. Kołodyńska, *Ecotoxicol. Environ. Saf.*, 2021, **219**, 112336.
4 A. Saravanan, P. S. Kumar, D.-V. N. Vo, P. R. Yaashikaa, S. Karishma, S. Jeevanantham, B. Gayathri and V. D. Bharathi, *Environ. Chem. Lett.*, 2021, **19**, 441–463.
5 Z. Gong, H. Chan, Q. Chen and H. Chen, *Nanomaterials*, 2021, **11**, 1792.
6 A. Hussain, S. Ashique, M. Z. Hassan, O. Afzal, Y. I. Asiri, P. Kumar, K. Dua, T. J. Webster, A. S. Altamimi and M. A. Altamimi, *J. Mol. Liq.*, 2023, **389**, 122905.
7 S. Zheng, Y. Yang, C. Wen, W. Liu, L. Cao, X. Feng, J. Chen, H. Wang, Y. Tang and L. Tian, *Environ. Int.*, 2021, **154**, 106555.
8 N. Munir, M. Jahangeer, A. Bouyahya, N. El Omari, R. Ghchime, A. Balahbib, S. Aboulaghras, Z. Mahmood, M. Akram and S. M. Ali Shah, *Sustainability*, 2021, **14**, 161.
9 B.-H. Yeo, T.-K. Tang, S.-F. Wong, C.-P. Tan, Y. Wang, L.-Z. Cheong and O.-M. Lai, *Front. Pharmacol.*, 2021, **12**, 631136.
10 Q. Liu, Z. Chen, Y. Chen, F. Yang, W. Yao and Y. Xie, *J. Agric. Food Chem.*, 2021, **69**, 10450–10468.
11 J. Wang and R. Zhuan, *Sci. Total Environ.*, 2020, **701**, 135023.
12 R. Al-Tohamy, S. S. Ali, F. Li, K. M. Okasha, Y. A.-G. Mahmoud, T. Elsamahy, H. Jiao, Y. Fu and J. Sun, *Ecotoxicol. Environ. Saf.*, 2022, **231**, 113160.
13 J. O. Osuoha, B. O. Anyanwu and C. Ejileugha, *J. Hazard. Mater. Adv.*, 2023, **9**, 100206.
14 R. Kumar, M. Qureshi, D. K. Vishwakarma, N. Al-Ansari, A. Kuriqi, A. Elbeltagi and A. Saraswat, *Case Stud. Chem. Environ. Eng.*, 2022, **6**, 100219.
15 C. Yan, Z. Qu, J. Wang, L. Cao and Q. Han, *Chemosphere*, 2022, **286**, 131870.
16 N. Başaran, D. Paslı and A. A. Başaran, *Food Chem. Toxicol.*, 2022, **159**, 112762.
17 M. Ding, D. Zhao, R. Wei, Z. Duan, Y. Zhao, Z. Li, T. Lin and C. Li, *Exploration*, 2024, **4**, 20230057.
18 B. Tian, S. Hua, Y. Tian and J. Liu, *Environ. Sci. Pollut. Res.*, 2021, **28**, 1317–1340.
19 M. A. Alnaqbi, A. Alzamly, S. H. Ahmed, M. Bakiro, J. Kegere and H. L. Nguyen, *J. Mater. Chem. A*, 2021, **9**, 3828–3854.
20 U. Schubert, *Chem. Soc. Rev.*, 2011, **40**, 575–582.
21 Q. Fu, Z.-Z. Xia, X. Sun, H.-L. Jiang, L.-L. Wang, S.-y. Ai and R.-S. Zhao, *TrAC, Trends Anal. Chem.*, 2023, **162**, 117054.
22 N. Stock and S. Biswas, *Chem. Rev.*, 2012, **112**, 933–969.
23 B.-E. Channab, M. El Ouardi, O. Ait Layachi, S. E. Marrane, A. El Idrissi, A. BaQais and H. Ait Ahsaine, *Environ. Sci.: Nano*, 2023, **10**, 2957–2988.
24 H.-C. Zhou, J. R. Long and O. M. Yaghi, *Chem. Rev.*, 2012, **112**, 673–674.
25 T. Hamoule, N. Mohammadi, B. Mousazadeh and H. Fakhari, *Int. J. Environ. Sci. Technol.*, 2023, **20**, 11913–11930.
26 A. Bhuyan and M. Ahmaruzzaman, *Next Sustainability*, 2024, **3**, 100016.
27 C. Piscopo, A. Polyzoidis, M. Schwarzer and S. Loebbecke, *Microporous Mesoporous Mater.*, 2015, **208**, 30–35.
28 X. Wang, J. Liu, S. Leong, X. Lin, J. Wei, B. Kong, Y. Xu, Z.-X. Low, J. Yao and H. Wang, *ACS Appl. Mater. Interfaces*, 2016, **8**, 9080–9087.
29 P.-H. Chang, R. Mukhopadhyay, B. Zhong, Q.-Y. Yang, S. Zhou, Y.-M. Tzou and B. Sarkar, *J. Colloid Interface Sci.*, 2023, **636**, 459–469.
30 K. Yue, X. Zhang, S. Jiang, J. Chen, Y. Yang, F. Bi and Y. Wang, *J. Mol. Liq.*, 2021, **335**, 116108.
31 S. Jiang, Z. Zhao, J. Chen, Y. Yang, C. Ding, Y. Yang, Y. Wang, N. Liu, L. Wang and X. Zhang, *Surf. Interfaces*, 2022, **30**, 101843.
32 R. Zhu, M. Cai, T. Fu, D. Yin, H. Peng, S. Liao, Y. Du, J. Kong, J. Ni and X. Yin, *Pharmaceutics*, 2023, **15**, 1599.
33 H. Zhao, Q. Li, Z. Wang, T. Wu and M. Zhang, *Microporous Mesoporous Mater.*, 2020, **297**, 110044.
34 Y.-X. Li, Y.-C. Han and C.-C. Wang, *Chem. Eng. J.*, 2021, **405**, 126648.
35 M. Simani and H. Dehghani, *Fuel*, 2024, **378**, 132942.
36 R. Nivetha, K. Gothandapani, V. Raghavan, G. Jacob, R. Sellappan, P. Bhardwaj, S. Pitchaimuthu, A. N. M. Kannan, S. K. Jeong and A. N. Grace, *ACS Omega*, 2020, **5**, 18941–18949.
37 S. Zhao, Y. Li, M. Wang, B. Chen, Y. Zhang, Y. Sun, K. Chen, Q. Du, Y. Wang and X. Pi, *Langmuir*, 2023, **39**, 10611–10624.
38 S.-K. Park, J. K. Kim and Y. C. Kang, *Chem. Eng. J.*, 2018, **334**, 2440–2449.
39 X. Zhao, P. Pachfule, S. Li, J. R. J. Simke, J. Schmidt and A. Thomas, *Angew. Chem.*, 2018, **130**, 9059–9064.
40 W. Liu, J. Zhou, L. Ding, Y. Yang and T. Zhang, *Chem. Phys. Lett.*, 2020, **749**, 137431.
41 N. Zurita-Méndez, G. Carbajal-De la Torre and M. Espinosa-Medina, *MRS Adv.*, 2024, **9**, 777–783.
42 K. Hemkumar, P. Ananthi and A. Pius, *Mater. Sci. Eng., B*, 2023, **292**, 116453.
43 E. Özcan and Y. Zorlu, *ChemistrySelect*, 2024, **9**, e202400471.
44 E. Rahmani and M. Rahmani, *Microporous Mesoporous Mater.*, 2017, **249**, 118–127.
45 S. Surblé, C. Serre, C. Mellot-Draznieks, F. Millange and G. Férey, *Chem. Commun.*, 2006, 284–286.
46 H. Liu, Y. Shao, S. Dou and C. Pan, *Sci. Energy Environ.*, 2024, 9.
47 C. Liu, W. Gong, T. Iftikhar, W. Liu, L. Su and X. Zhang, *Next Mater.*, 2025, **7**, 100362.

48 C. Li, Y. Yuan, M. Yue, Q. Hu, X. Ren, B. Pan, C. Zhang, K. Wang and Q. Zhang, *Small*, 2024, **20**, 2310373.
49 D. Li, Y. Hao, H. Zhou, W. Ma, N. Zhang and M. Lu, *Chem. Eng. J.*, 2025, **507**, 160784.
50 Y. L. Liu, X. J. Zhao, X. X. Yang and Y. F. Li, *Analyst*, 2013, **138**, 4526–4531.
51 A. Abdulla, MS thesis, The University of Western Ontario, Canada, 2017.
52 J. Amaro-Gahete, R. Klee, D. Esquivel, J. R. Ruiz, C. Jiménez-Sanchidrián and F. J. Romero-Salguero, *Ultrason. Sonochem.*, 2019, **50**, 59–66.
53 J. F. Kurisingal, Y. Rachuri, Y. Gu, Y. Choe and D.-W. Park, *Inorg. Chem. Front.*, 2019, **6**, 3613–3620.
54 N. Hassan, A. Shahat, I. El-Deen, M. El-Afify and M. El-Bindary, *J. Mol. Struct.*, 2022, **1258**, 132662.
55 S.-N. Kim, C. G. Park, B. K. Huh, S. H. Lee, C. H. Min, Y. Y. Lee, Y. K. Kim, K. H. Park and Y. B. Choy, *Acta Biomater.*, 2018, **79**, 344–353.
56 D. Han, L. Hao, M. Chang, J. Dong, Y. Gao and Y. Zhang, *J. Colloid Interface Sci.*, 2023, **634**, 14–21.
57 J. Yuan, H. Duan, L. Wang, S. Wang, Y. Li and J. Lin, *Food Chem.*, 2023, **408**, 135212.
58 J. Hua, F.-y. Chen, Y.-b. Tang, S.-g. Zhao, J.-t. Yang and R. Wu, *J. Phys. Chem. Solids*, 2023, **177**, 111299.
59 M. Chen, P. Chen, Z. Ji, M. Yu, J. Tan, B. Fu and X. Zhu, *ACS Omega*, 2023, **8**, 13323–13331.
60 N. Kitchamsetti and D. Kim, *J. Alloys Compd.*, 2023, **959**, 170483.
61 D. A. Nurani, N. Anisa, I. Khatrin, Yasmine, G. T. Kadja and Y. K. Krisnandi, *Chemistry*, 2024, **6**, 283–298.
62 S. A. Mohammadi, H. Najafi, N. Asasian-Kolur, A. E. Pirbazari and S. Sharifian, *J. Mol. Liq.*, 2024, **405**, 125119.
63 T. Nasiriani, N. A. Nigjeh, S. Torabi and A. Shaabani, *Carbohydr. Polym.*, 2024, **342**, 122418.
64 Z. Tang, L. Hao, M. Hu, Y. Gao and Y. Zhang, *J. Alloys Compd.*, 2024, **1005**, 176155.
65 Z. U. Zango, N. H. H. A. Bakar, N. S. Sambudi, K. Jumbri, N. A. F. Abdullah, E. A. Kadir and B. Saad, *J. Environ. Chem. Eng.*, 2020, **8**, 103544.
66 I. Gholamali and M. Yadollahi, *Int. J. Biol. Macromol.*, 2025, **290**, 139044.
67 J. Dong, W. Liu, B. An, H. Su, L. Zhang, N. Li, Y. Gao and L. Ge, *Sep. Purif. Technol.*, 2024, **342**, 127017.
68 S. Chaemchuen, Z. Luo, K. Zhou, B. Mousavi, S. Phatanasri, M. Jaroniec and F. Verpoort, *J. Catal.*, 2017, **354**, 84–91.
69 L. Lu, Q. Xu, Y. Chen, Y. Zhou, T. Jiang and Q. Zhao, *J. Energy Storage*, 2022, **49**, 104073.
70 P. Azari, H. Hasheminejad and K. Zarean Mousaabadi, *Sci. Rep.*, 2025, **15**, 8503.
71 J. Guo, Y. Gao, X. Cao, L. Li, X. Yu, S. Chi, H. Liu, G. Tian and X. Zhao, *Renewable Energy*, 2025, 122661.
72 W. Jin, R. Wang and X. Huang, *J. Mol. Liq.*, 2020, **312**, 113442.
73 Y. Huo, S. Xiu, L.-Y. Meng and B. Quan, *Chem. Eng. J.*, 2023, **451**, 138572.
74 Y. Han, P. Mu, J. Wang and D. Qi, *Forests*, 2023, **14**, 1772.
75 X. Liao, F. Wang, F. Wang, Y. Cai, Y. Yao, B.-T. Teng, Q. Hao and L. Shuxiang, *Appl. Catal., B*, 2019, **259**, 118064.
76 Z. Zhao, H. Li, K. Zhao, L. Wang and X. Gao, *Chem. Eng. J.*, 2022, **428**, 131006.
77 A. Arenas-Vivo, D. Avila and P. Horcajada, *Materials*, 2020, **13**, 1469.
78 M. Y. Zorainy, S. Kaliaguine, M. Gobara, S. Elbasuney and D. C. Boffito, *J. Inorg. Organomet. Polym. Mater.*, 2022, **32**, 2538–2556.
79 G. Zanchettin, G. da Silva Falk, S. Y. G. González and D. Hotza, *Chem. Eng. Process.*, 2021, **166**, 108438.
80 X. Cheng, J. Zhou, J. Chen, Z. Xie, Q. Kuang and L. Zheng, *Nano Res.*, 2019, **12**, 3031–3036.
81 X. Liu, W. Qi, Y. Wang, R. Su and Z. He, *Eur. J. Inorg. Chem.*, 2018, **2018**, 4579–4585.
82 Y. T. Dang, H. T. Hoang, H. C. Dong, K.-B. T. Bui, L. H. T. Nguyen, T. B. Phan, Y. Kawazoe and T. L. H. Doan, *Microporous Mesoporous Mater.*, 2020, **298**, 110064.
83 S. Sumitomo, H. Koizumi, M. A. Uddin and Y. Kato, *Ultrason. Sonochem.*, 2018, **40**, 822–831.
84 M. Abbasian and M. Khayyatalimohammadi, *Int. J. Biol. Macromol.*, 2023, **234**, 123665.
85 Z. Liu, J. Wang, S. Dong, L. Wang, L. Li, Z. Cao, Y. Zhang, L. Cheng and J. Yang, *Ultrason. Sonochem.*, 2024, **107**, 106912.
86 S. Abdpour, E. Kousari, M. M. Alavi and B. Bazri, *International Conference on Engineering & Applied Sciences*, UAE - DUBAI, 2016.
87 S. Li, T. Zhang, H. Zheng, X. Dong, Y. K. Leong and J.-S. Chang, *Sci. Total Environ.*, 2024, 171885.
88 L. Wang, T. Luo, J. Jiao, G. Liu, B. Liu, L. Liu and Y. Li, *Sep. Purif. Technol.*, 2024, **329**, 125091.
89 F. Fu and Q. Wang, *J. Environ. Manage.*, 2011, **92**, 407–418.
90 Z. Wang, Y. Li, J. Peng, H. Song and C. Chen, *J. Water Process Eng.*, 2025, **69**, 106842.
91 Z. U. Zango, K. Jumbri, N. S. Sambudi, N. H. H. A. Bakar, N. A. F. Abdullah, C. Basheer and B. Saad, *RSC Adv.*, 2019, **9**, 41490–41501.
92 S. Ghazali, A. Baalbaki, W. B. Karroum, A. Bejjani and A. Ghauch, *Environ. Sci.: Adv.*, 2024, **3**, 119–131.
93 J.-B. Huo and G. Yu, *Int. J. Mol. Sci.*, 2022, **23**, 14556.
94 M. Bakhtian, N. Khosroshahi and V. Safarifard, *ACS Omega*, 2022, **7**, 42901–42915.
95 R. Dou, J. Zhang, Y. Chen and S. Feng, *Environ. Sci. Pollut. Res.*, 2017, **24**, 8778–8789.
96 J. Imanipoor, M. Mohammadi, M. Dinari and M. R. Ehsani, *J. Chem. Eng. Data*, 2020, **66**, 389–403.
97 K. P. Gopinath, D.-V. N. Vo, D. Gnana Prakash, A. Adithya Joseph, S. Viswanathan and J. Arun, *Environ. Chem. Lett.*, 2021, **19**, 557–582.
98 F. Hajibabaei, S. S. Movafagh, S. Salehzadeh and R. W. Gable, *Dalton Trans.*, 2023, **52**, 7031–7047.
99 S. Karimi and H. Namazi, *Chemosphere*, 2024, **352**, 141397.
100 P. Calza, V. Sakkas, C. Medana, C. Baiocchi, A. Dimou, E. Pelizzetti and T. Albanis, *Appl. Catal., B*, 2006, **67**, 197–205.

101 A. A. Alluhaybi, A. Alharbi, K. F. Alshammari and M. G. El-Desouky, *ACS Omega*, 2023, **8**, 40775–40784.
102 E. Chiani, S. Ghasemi and S. N. Azizi, *ACS Omega*, 2024, **9**, 26983–27001.
103 S. Wu, H. Min, W. Shi and P. Cheng, *Adv. Mater.*, 2020, **32**, 1805871.
104 Y. A. Ghorbani, S. M. Ghoreishi and M. Ghani, *Polycyclic Aromat. Compd.*, 2022, **42**, 5496–5507.
105 L.-J. Wang, W. Han, T.-T. Lou, L.-L. Ma, Y.-B. Xiao, Z. Xu, M.-L. Chen, Y.-H. Cheng and L. Ding, *Anal. Methods*, 2023, **15**, 343–352.
106 J. H. Cho, J. Ma and S. Y. Kim, *Exploration*, 2023, **3**, 20230001.
107 W. Wu, Y. Li, P. Song, Q. Xu, N. Long, P. Li, L. Zhou, B. Fu, J. Wang and W. Kong, *Trends Food Sci. Technol.*, 2023, **138**, 238–271.
108 W. Zhang, X. Li, X. Ding, K. Hua, A. Sun, X. Hu, Z. Nie, Y. Zhang, J. Wang and R. Li, *RSC Adv.*, 2023, **13**, 10800–10817.
109 H. Liu, L. Jiang, S. Huang, J. Niu, Y. Zhang, J. Liao, G. Dong, D. Song and Q. Zhou, *J. Chromatogr. A*, 2025, **1740**, 465560.
110 R. Guo, L. Xue, G. Cai, W. Qi, Y. Liu and J. Lin, *ACS Appl. Nano Mater.*, 2021, **4**, 5115–5122.
111 M. Hu, Y. Wang, J. Yang, Y. Sun, G. Xing, R. Deng, X. Hu and G. Zhang, *Biosens. Bioelectron.*, 2019, **142**, 111554.
112 X. Jiang, W. Su, W. Shi and H. Wang, *Anal. Methods*, 2024, **16**, 8333–8340.
113 M. Lian, Y. Shi, L. Chen, Y. Qin, W. Zhang, J. Zhao and D. Chen, *ACS Sens.*, 2022, **7**, 2701–2709.
114 J. Xu, X. Zhang, J. Zhong, S. Huang, S. Wang and H. Zhai, *Spectrochim. Acta, Part A*, 2024, **316**, 124315.
115 C. Zhao, Z. Jiang, R. Mu and Y. Li, *Talanta*, 2016, **159**, 365–370.
116 X. Wang, Y. Yun, W. Sun, Z. Lu and X. Tao, *Sens. Actuators, B*, 2022, **353**, 131143.
117 J. Yuan, L. Wang, H. Duan, S. Ye, Y. Ding, Y. Li and J. Lin, *Food Chem.*, 2025, **467**, 142343.
118 K. Ren, Y. Li and Q. Liu, *Anal. Chim. Acta*, 2025, **1336**, 343523.
119 Y. Zhang, W. Zhang, K. Chen, Q. Yang, N. Hu, Y. Suo and J. Wang, *Sens. Actuators, B*, 2018, **262**, 95–101.
120 M. Fu, B. Chai, J. Yan, C. Wang, G. Fan, G. Song and F. Xu, *Appl. Phys. A: Mater. Sci. Process.*, 2021, **127**, 928.
121 Z. Li, F. Meng, R. Li, Y. Fang, Y. Cui, Y. Qin and M. Zhang, *Biosens. Bioelectron.*, 2023, **234**, 115294.
122 S. Duan and Y. Huang, *J. Electroanal. Chem.*, 2017, **807**, 253–260.
123 P. Chen, Z. Liu, J. Liu, H. Liu, W. Bian, D. Tian, F. Xia and C. Zhou, *Electrochim. Acta*, 2020, **354**, 136644.
124 R. Han, Y. Sun, Y. Dai, D. Gao, X. Wang and C. Luo, *Sens. Actuators, B*, 2021, **326**, 128833.
125 H. Chen, K. Luo, Q. Zhou, Z. Yan and K. Li, *Microchem. J.*, 2020, **158**, 105249.
126 Y. Liu, X.-Z. Meng, X. Luo, H.-W. Gu, X.-L. Yin, W.-L. Han, H.-C. Yi and Y. Chen, *Sens. Actuators, B*, 2024, **410**, 135682.
127 D. K. Yadav, V. Ganesan, R. Gupta, M. Yadav and P. K. Rastogi, *J. Chem. Sci.*, 2020, **132**, 1–8.
128 R. T. Massah, S. L. Zambou Jiokeng, J. Liang, E. Njanja, T. M. Ma Ntep, A. Spiess, L. Rademacher, C. Janiak and I. K. Tonle, *ACS Omega*, 2022, **7**, 19420–19427.
129 L. Gong, S. Jin, R. Liu, Z. Liu, Y. Zhang, L. Zhang, T. Zhao, H. Fa and W. Yin, *Microchem. J.*, 2024, **205**, 111262.
130 Y.-H. Sun, L. Yang, X.-X. Ji, Y.-Z. Wang, Y.-L. Liu, Y. Fu and F. Ye, *Food Chem.*, 2024, **440**, 138244.
131 W. Jiang, W. Liang, C. Zhao, W. Lai, B. Cong, S. Zhang, M. Jiang, H. Li and C. Hong, *Sens. Actuators, B*, 2024, **407**, 135498.
132 H. Zhu, S. Chen, X. Huang, X. Chen and Z. Gong, *Anal. Chim. Acta*, 2024, **1330**, 343274.
133 H. Dai, J. Yu, R. Zhou, G. Hao, Z. Qiao, Z. Feng, X. Liu, J. Bi, J. Wang and X. Liu, *Food Chem.*, 2025, 143378.
134 J. Li, L. Li, P. Zhao and Y. Xie, *Microchem. J.*, 2024, **200**, 110426.
135 J. Zhao, H. Wang, Z.-k. He, W. Zhang, Y. Du, X. Li, S. Wang, J. Zhao, Y.-Y. Song and Z. Gao, *ACS Sens.*, 2024, **9**, 4166–4175.
136 Y. Yang, J. Yue, X. Zhang, B. Ren, S. Fu, Y. Sun and Z. Luo, *Ceram. Int.*, 2024, **50**, 38253–38262.
137 J. Han, F. Li, M. Zhao, M. Guo, Y. Liu, X. Guo, Q. Ran, Z. Wang and H. Zhao, *Microchem. J.*, 2024, **200**, 110323.
138 Y. Yu, S. Zeng, X. Wen and W. Qiu, *Microchem. J.*, 2025, 113778.
139 J. Ru, X. Wang, Z. Zhou, J. Zhao, J. Yang, X. Du and X. Lu, *Anal. Chim. Acta*, 2022, **1195**, 339451.
140 R. Liu, C. Zhang, T. Wu, R. Liu, Y. Sun and J. Ma, *Talanta*, 2024, **273**, 125882.
141 F. Jahangiri-Dehaghani, H. R. Zare and Z. Shekari, *Talanta*, 2024, **266**, 124947.
142 J. Li, L. Qu, H. Li, L. Zhao, T. Chen, J. Liu, Y. Gao and H. Pan, *Microchim. Acta*, 2023, **190**, 366.
143 J. Zhang, Y. Zeng, L. Chen, X. Lei, Y. Yang, Z. Chen, L. Guo and L. Li, *Environ. Res.*, 2023, **225**, 115499.
144 X. Wang, X. Xu, T. Zhou and T. Zhang, *Sens. Actuators, B*, 2024, **413**, 135874.
145 Z. Ma, Y. Zhang, T. Yuan, Y. Fan, X. Wang, Z. Xue, A. Zhong and J. Xu, *J. Hazard. Mater.*, 2025, **486**, 136859.
146 A. Das, O. Ali, S. Paul, A. Jana and A. Bhunia, *Inorg. Chim. Acta*, 2024, **570**, 122163.
147 W. Xu, Y. Zhao, F. Gao, X. Zheng, F. Zhan and Q. Wang, *Bioelectrochemistry*, 2025, **165**, 108965.
148 H. Wang, X. Jia, Z. Ma, X. Wang, X. Zhang, Z. Xue and J. Xu, *Sens. Actuators, B*, 2024, **404**, 135204.
149 T. Van Tran, A. Jalil, D. T. C. Nguyen, M. Alhassan, W. Nabgan, A. N. T. Cao, T. M. Nguyen and D.-V. N. Vo, *Environ. Res.*, 2023, **216**, 114422.
150 D. Ren, X. Wang, C. Leng, W. Meng, J. Zhang and C. Han, *J. Electrochem. Soc.*, 2022, **169**, 097501.
151 A. K. Pandey, M. K. Samota, A. Kumar, A. S. Silva and N. K. Dubey, *Front. Sustain. Food Syst.*, 2023, **7**, 1162595.
152 L.-H. Yu, Y.-H. Pang and X.-F. Shen, *Food Chem.*, 2025, **476**, 143482.
153 Y. Fan, B. Hou, F. Lu, D. Liu and X. Cui, *Food Chem.*, 2025, **465**, 142148.

154 X. Liu, T. Liang, R. Zhang, Q. Ding, S. Wu, C. Li, Y. Lin, Y. Ye, Z. Zhong and M. Zhou, *ACS Appl. Mater. Interfaces*, 2021, **13**, 9643–9655.
155 L. E. Chiñas-Rojas, J. E. Domínguez, L. Á. A. Herrera, F. E. González-Jiménez, R. Colorado-Peralta, J. A. Arenzano Altaif and J. M. Rivera Villanueva, *ChemMedChem*, 2024, **19**, e202400144.
156 N. Salandari-Jolge, A. A. Ensafi and B. Rezaei, *Anal. Bioanal. Chem.*, 2021, **413**, 7451–7462.
157 S. Darvishi, S. Javanbakht, A. Heydari, F. Kazeminava, P. Gholizadeh, M. Mahdipour and A. Shaabani, *Int. J. Biol. Macromol.*, 2021, **181**, 937–944.
158 Y. Wang, D. Ren, Y. Zhang, J. Li, W. Meng, B. Tong, J. Zhang, C. Han and L. Dai, *Anal. Chim. Acta*, 2023, **1283**, 341936.
159 C. Gao, H. Zhu, J. Chen and H. Qiu, *Chin. Chem. Lett.*, 2017, **28**, 1006–1012.
160 Q. Jiang, Y. Xiao, A. N. Hong, Z. Gao, Y. Shen, Q. Fan, P. Feng and W. Zhong, *ACS Appl. Mater. Interfaces*, 2022, **14**, 41800–41808.